LINC00847 drives pancreatic cancer progression by targeting the miR-455-3p/HDAC4 axis

Shunxin Hao, Zhi Yao, Yifeng Liu

Department of General Surgery, Wuhan University of Science and Technology Hospital, Wuhan, Hubei, China

Submitted: 11 May 2023; **Accepted:** 29 August 2023
Online publication: 30 June 2024

Arch Med Sci 2024; 20 (3): 847–862
DOI: https://doi.org/10.5114/aoms/171672

Corresponding author:
Yifeng Liu
Department of General Surgery
Wuhan University of Science and Technology Hospital
No. 2 Huangjiahu West Road
Hongshan District
Wuhan 430065
Hubei, China
Phone/fax: +86 13397189538
E-mail: yifengliuLYF@163.com

Abstract

Introduction: Pancreatic cancer (PC) is a common malignant tumor of the digestive system, posing a serious threat to the life of patients. This study aims to investigate the role of LINC00847 and the LINC00847/miR-455-3p/HDAC4 mechanism in PC progression.

Material and methods: The RNA levels of LINC00847, miR-455-3p and HDAC4 were determined by RT-qPCR. HDAC4 protein level was assessed by western blotting. Colony formation and CCK-8 assays were employed to test the proliferation of PC cells. Transwell and scratch assays were conducted to evaluate the cell invasive and migratory abilities, respectively. The effect of LINC00847 silencing on PC cells *in vivo* was verified using a mouse xenograft model. The correlation among LINC00847, miR-455-3p and HDAC4 was ascertained by dual-luciferase reporter (DLR) assay and Pearson's correlation analysis.

Results: The result showed that LINC00847 mainly localized in the cytoplasm was upregulated in PC cells and tissues. Downregulating LINC00847 hindered migration, proliferation, and invasion of PC cells *in vitro*. Moreover, it also suppressed tumor growth in an *in vivo* xenograft model. LINC00847 was found to directly target miR-455-3p. miR-455-3p overexpression inhibited cell proliferation and invasion. In addition, HDAC4 was confirmed to be a target gene of miR-455-3p, and HDAC4 overexpression overturned the impact of LINC00847 knockdown on PC cell progression.

Conclusions: Our findings reveal that LINC00847 potentially plays a key role in the carcinogenesis of PC progression. This effect may be mediated via regulating the miR-455-3p/HDAC4 axis. This study provides insights into the intricate molecular mechanisms underlying PC and opens avenues for potential therapeutic interventions.

Key words: pancreatic cancer, LINC00847, miR-455-3p, HDAC4.

Introduction

The incidence of pancreatic cancer (PC) is increasing each year, and it is an aggressive cancer that affects the digestive system. Over 490,000 new PC cases were identified in 2020, and 460,000 PC deaths occurred globally [1]. Currently, surgery is still a common form of treatment for PC, but it comes with a significant risk of postoperative recurrence and metastasis [2]. Due to the insidious onset and high degree of malignancy of PC, 80% to 85% of patients lose the chance of surgical resection after diagnosis [3]. Therefore, there is an urgent need to explore the mech-

anism of PC to find molecular markers for early diagnosis, prognosis and novel targets for therapy.

Long non-coding RNAs (lncRNAs) have been considered as 'junk DNA' in the past due to the lack of a complete open reading frame and no protein-coding function [4]. With the in-depth research on molecular biology, the potential biological functions of lncRNAs have been continuously explored. Many studies have revealed that lncRNAs have a substantial function in the progression of several tumor cells, together with PC [5, 6]. LncRNA CYTOR accelerated the malignancy of PC by facilitating cell growth and migration [7]. Zhang *et al.* reported that lncRNA LINK-A promoted the development of early-stage PC by increasing ROCK1 expression [8]. Here, we used the GEPIA database to find that Long intergenic nonprotein coding RNA 847 (LINC00847) was upregulated in pancreatic adenocarcinoma samples. After checking the literature, LINC00847, a newly discovered lncRNA, was reported to contribute to non-small cell lung cancer progression [9] and hepatocellular carcinoma progression [10]. Nevertheless, there is no information available on LINC00847's precise PC function.

LncRNAs, as competitive endogenous RNAs (ceRNAs), can interact with microRNAs (miRNAs) to affect the incidence and progression of tumors [11, 12]. MiR-455-3p can interact with lncRNA to take part in the development of many tumors. By way of illustration, miR-455-3p sponged by LINC00472 could worsen the progression of oral squamous cell carcinoma [13]. Oppositely, miR-455-3p interacted with LINC00319 to suppress osteosarcoma progression [14]. In PC, Zhan *et al.* confirmed that miR-455-3p restrained PC tumor progression by suppressing the TAZ and Wnt/β-catenin pathway [15]. Nevertheless, the interaction between miR-455-3p and LINC00847 in PC progression remains unknown.

In the current study, we investigated the expression and functional role of LINC00847 in PC progression by molecular biological approaches. We found that knockdown of LINC00847 regulated tumor progression by blocking miR-445-3p and increasing histone deacetylase 4 (HDAC4).

Based on our findings, we highlighted the potential of LINC00847 as a therapeutic target for PC.

Material and methods

Tissue specimens and cell lines

Clinical samples could be taken from Wuhan University of Science and Technology Hospital with the approval of its ethics committee. No patients had undergone medical therapy or radiation previous to surgery, and all of them had PC that was pathologically confirmed. A total of 35 PC specimens and paired adjacent non-tumor specimens were collected and stored in a –80°C refrigerator. Before obtaining tissues samples, the patients were informed and signed the informed consent.

The BeNa Culture Collection provided the PC cell line (Capan-1) as well as the human pancreatic normal ductal epithelial cell (HPDE) cell line. The other PC cell lines (HuP-T3 and PSN-1) were obtained from Beijing Zhongyuan Ltd. (China). PSN-1 and HPDE cells were grown in RPMI-1640 media with 10% FBS from Procell (China), Capan-1 cells were cultured in IMDM medium with 20% FBS from Procell, and HuP-T3 cells were cultivated in MEM medium with 10% FBS from Procell. Cells were incubated in a constant temperature incubator (37°C, 5% CO_2).

Cell transfection

Two small interfering RNAs (siRNA) targeting LINC00847 (si-LINC00847-1 and si-LINC00847-2), the siRNA negative control (si-NC), the miR-455-3p mimic, the mimic negative control (mimic-NC), the HDAC4 overexpression vector (HDAC4-OE), and the empty vector as the negative control of overexpression vector were synthesized by GenePharma (Shanghai, China). Capan-1 and PSN-1 cells (4×10^5 cells/well) were cultured on a 6-well plate under the following conditions: 37°C and 5% CO_2. When the cell confluence was more than 60%, the vectors mentioned above were transfected into Capan-1 and PSN-1 cells using Lipofectamine 3000 (Thermo Fisher, USA) according to the instructions. After 48 h of cell transfection, the transfection efficiency for each vector was evaluated by RT-qPCR.

RT-qPCR

Total RNA was extracted from tissues as well as cells using Trizol (Invitrogen, USA). Briefly, 1 ml of Trizol was added into tissues and cells for 5 min of quiescence. After centrifugation at 12 000× g for 15 min at 4°C, 0.2 ml of chloroform was added to the isolated RNA in the supernatant for 3 min quiescence, then RNA was precipitated using 0.5 ml of isopropanol for 10 min quiescence, and finally purified using 1 ml of 75% ethyl alcohol for 10 min quiescence. The isolated RNA was dissolved in RNase-free H_2O, the RNA concentration was detected using the ratio of OD260 to OD280, and the quality of total RNA was confirmed using agarose electrophoresis. The TIANScript II RT Kit (TIANGEN, China) reverse-transcribed 500 ng of RNA into cDNA. For qPCR amplification, Genious 2× SYBR Green Fast qPCR Mix (ABclonal Technology Co., Ltd., China) was utilized with the following conditions: 95°C for 3 min, and 40 cycles of 95°C

Table I. Primer sequences

Gene		Primers 5′-3′
LINC00847	Forward	5′- AACGCTGCCTCTGTGGAAGTCTC-3′
	Reverse	5′- CGCTCTGCTCTCCCGCCATC-3′
miR-455-3p	Forward	5′- TGCGCCAAACCACACTGTGGTG-3′
	Reverse	5′- CCAGTGCAGGGTCCGAGGTATT-3′
HDAC4	Forward	5′- AACGCTTCACGAATT TGCGT-3′
	Reverse	5′-GTGAGAACTGGTGGTCCAGG-3′
GAPDH	Forward	5′- GAGTCAACGGATTTGGTCGT-3′
	Reverse	5′- TGGGTGGAATCATATTGGAA-3′
U6	Forward	5′- CTCGCTTCGGCAGCACA-3′
	Reverse	5′- AACGCTTCACGAATT TGCGT-3′

for 5 s and 60°C for 30 s. The $2^{-\Delta\Delta Ct}$ method was used to calculate the relative levels of LINC00847, HDAC4 and miR-455-3p after normalizing to GAPDH and U6. The primer sequences are depicted in Table I.

Nuclear and cytoplasmic RNA fractionation

Nuclear and cytoplasmic RNA was extracted from Capan-1, PSN-1 cells by the Minute Cytoplasmic and Nuclear Fractionation kit (Invent, USA). The distribution of LINC00847 in the cytoplasm and nucleus was measured by RT-qPCR with the references of GAPDH and U6.

Cell counting kit 8 (CCK-8) assay

The digested and resuspended cells were in the logarithmic phase. Following dilution, 96-well plates were seeded with a 100 µl cell suspension (3000 cells per well). Each well received 10 µl of CCK-8 reagent (Beyotime, China) at a separate time (0, 24, 48, 72, and 96 h). A microplate reader measured the absorbance value of each well at 450 nm after 2 h of incubation (TECAN, Switzerland).

Colony formation assay (CFA)

Six-well plates received an injection of 500 cells, which were then grown at 37 °C and 5% CO_2. Cells were fixed (4% paraformaldehyde for 10 min) and stained after 2 weeks (0.1% crystal violet for 15 min). The number of colonies was counted and photographed with a microscope.

Transwell assay

The surface of the top Transwell chamber (Corning, USA) was coated with 50 mg/µl Matrigel dilution (Biosciences, USA). Cell suspension (2×10^5 cells/well) without FBS was inoculated into the upper chamber of the Transwell, and in the lower compartment, 600 µl of 10% FBS media was added. The cells were fixed with 4% paraformaldehyde and stained with crystal violet after 48 h of incubator culture. An inverted microscope (Olympus, Japan) was used to capture images of five randomly chosen fields from each well, after which the number of cells was determined.

Scratch test

5×10^5 cells were inoculated on a 6-well plate and cultured at 37°C for 24 h. When the cell confluence was more than 90%, the cells were scratched vertically with the 10 µl tip. After 0 h and 48 h, the plate was placed under the microscope and photographed. ImageJ software was used to calculate the scratch healing rate.

Dual-luciferase reporter (DLR) assay

The mutant-type and wild-type 3′UTR fragments of LINC00847 and HDAC4 were inserted into pGL3 vectors to construct mutant-type and wild-type of LINC00847 (LINC00847-MUT, LINC00847-WT) and HDAC4 (HDAC4-WT, HDAC4-MUT), respectively. LINC00847-WT, LINC00847-MUT, HDAC4-WT, and HDAC4-MUT were co-cultured with miR-455-3p mimic and mimic-NC by Lipofectamine 3000 (Thermo Fisher, USA). After a 48-hour incubator culture, each group's luciferase activity was measured using a dual-luciferase reporter gene detection kit (TransGen Biotech, China).

Western blot assay

The total protein was collected by RIPA lysate (Solarbio, China). The presence of protein was measured using the BCA Protein Assay Kit (Beyotime, China). The protein samples were electrophoresed on SDS-PAGE gels, transferred to PVDF membranes (Millipore, USA), and then blocked for a period of 1 to 2 h at room temperature with non-fat milk (5%). After that, the membrane was

treated at 4 °C overnight with primary antibodies (anti-HDAC4, 1 : 1000, ab12172, Abcam, USA; anti-GAPDH, 1 : 3000, ab9485, Abcam). The secondary antibody (anti-rabbit IgG/HRP, 1 : 5000, ab205718, Abcam) was then applied to the membrane and left at room temperature for 1 h. ECL illuminating solution from Millipore (USA) was then used to see the bands.

Xenograft mouse model

Five-week-old female BALB/C nude mice were acquired from our hospital's animal laboratory. The nude mice were kept in the animal room with constant temperature and humidity and no specific pathogens. Mice's left forelimb was subcutaneously injected with sh-LINC00847 or sh-NC, which had been introduced to PSN-1 cells in the lentivirus vector. Every 4 days, the tumor volumes in every group were measured using a vernier caliper and calculated with the following formula: tumor volume = short diameter^2 × long diameter/2. The mice were euthanized using pentobarbital sodium after 28 days of consuming a normal diet. The tumors were taken out, weighed, and captured on camera. The Animal Ethics Committee of Wuhan University of Science and Technology Hospital gave its approval for the animal experiment.

Statistical analysis

SPSS22.0 software (IBM, USA) was used for statistical analysis, and all data from three independent experiments were shown as mean ± standard deviation. The *t*-test was performed to analyze the statistical significance of differences between two groups, whereas one-way ANOVA was used to analyze the statistical significance of variation among multiple groups. The relationships among LINC00847, miR-22-3p and HDAC4 were confirmed by Pearson's correlation analysis. A *p*-value less than 0.05 indicates statistical significance.

Results

LINC00847 expression level is overexpressed in PC

According to the data from GEPIA, LINC00847 expression was found to be upregulated in pancreatic adenocarcinoma (PAAD) samples (Figure 1 A). Then, LINC00847 expression in PC tissues and cells was verified utilizing RT-qPCR. In comparison with non-tumor tissues using the t-test, elevated LINC00847 was verified in PC tissues ($p < 0.0001$, Figure 1 B). Similarly, LINC00847 was overexpressed in HuP-T3, Capan-1 and PSN-1 cells compared with HPDE cells using one-way ANOVA ($p < 0.001$, Figure 1 C). Additionally, LINC00847 was mainly localized in the cytoplasm (Figure 1 D). Therefore, our data indicated that LINC00847 is overexpressed in PC and may be involved in PC progression.

Knockdown of LINC00847 decreases cell growth of Capan-1 and PSN-1 cells

To evaluate the function of LINC00847 in PC progression, si-RNAs of LINC00847 were co-expressed into Capan-1 as well as PSN-1 cells to reduce the LINC00847 level. Results of RT-qPCR demonstrated that si-LINC00847-1 and si-LINC00847-2 both successfully depleted LINC00847 expression compared to si-NC using one-way ANOVA ($p < 0.001$, Figure 2 A). Through CCK-8 detection, the proliferation ability of Capan-1 and PSN-1 cells with si-LINC00847 was notably blocked compared to the si-NC group using one-way ANOVA ($p < 0.001$, Figure 2 B). Additionally, LINC00847 silencing suppressed the clonogenic ability of Capan-1 and PSN-1 cells compared to si-NC using one-way ANOVA ($p < 0.001$, Figure 2 C). All findings indicated that knockdown of LINC00847 blocked cell growth of PC cells.

Knockdown of LINC00847 hinders cell invasion and migration of Capan-1 and PSN-1 cells

To examine how LINC00847 affected Capan-1 and PSN-1 cells' capacity for invasion and migration, transwell and scratch assays were used. Capan-1 and PSN-1 cells' capacity to migrate was considerably inhibited when LINC00847 was knocked down as opposed to the si-NC group using one-way ANOVA ($p < 0.001$, Figure 3 A). Additionally, the capacity of Capan-1 and PSN-1 cells to invade was observed to be inhibited by LINC00847 silencing ($p < 0.001$ using one-way ANOVA, Figure 3 B). These findings suggested that LINC00847 knockdown prevented PC cells from migrating and invading.

Knockdown of LINC00847 decreases tumor growth *in vivo*

Animal tests were conducted to confirm that LINC00847 silencing had a tumor-suppressing impact. First, in nude mice, sh-LINC00847 was able to successfully reduce LINC00847 expression ($p < 0.001$ using *t*-test, Figure 4 A). The sh-LINC00847 group tumor volume was reduced as compare to the sh-NC group using the *t*-test ($p < 0.001$, Figures 4 B and C). Additionally, the sh-LINC00847 group's tumor weight was lower than the sh-NC group ($p < 0.001$ using *t*-test, Figure 4 D). Therefore, it was demonstrated that LINC00847 knockdown inhibits tumor development *in vivo*.

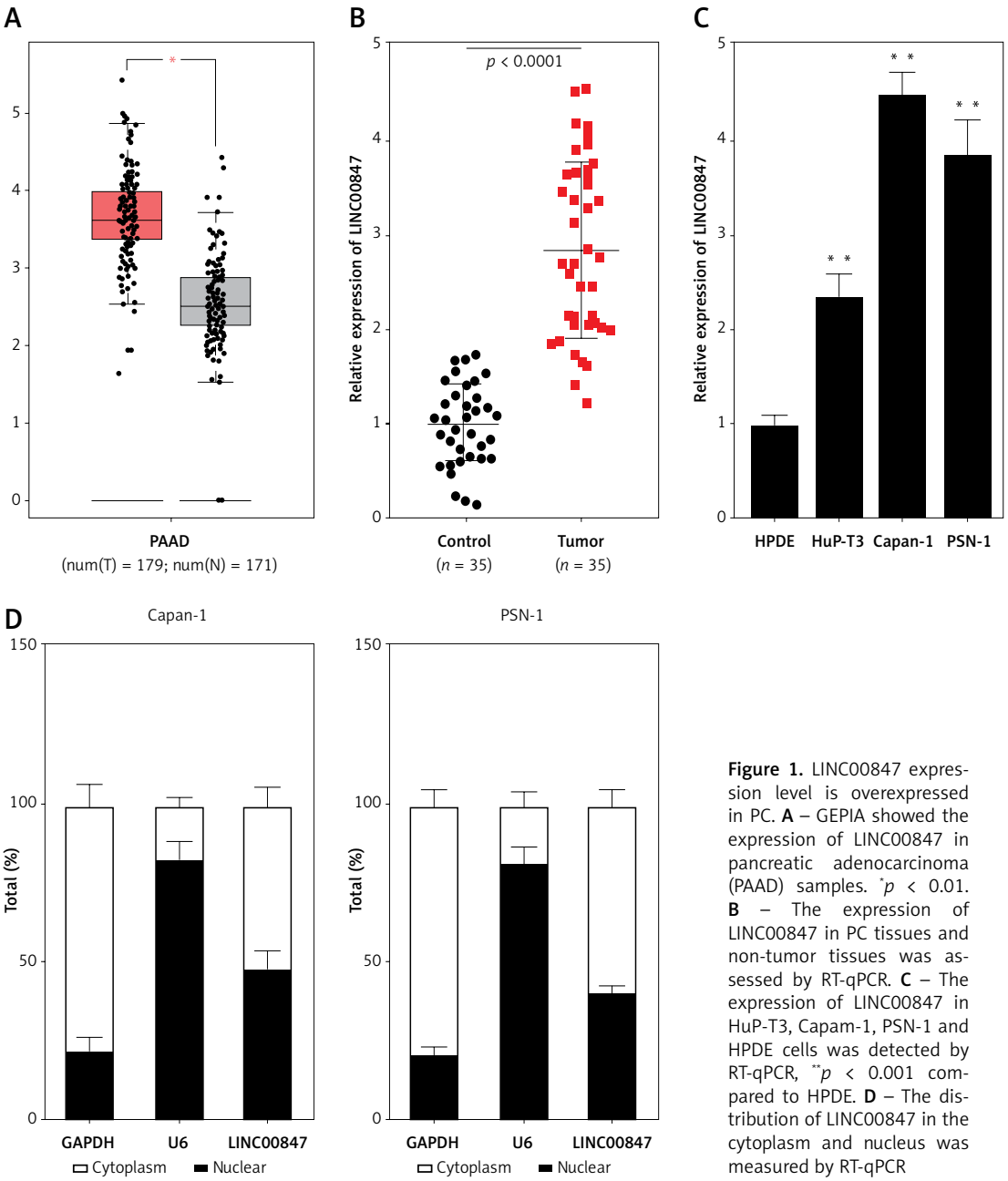

Figure 1. LINC00847 expression level is overexpressed in PC. **A** – GEPIA showed the expression of LINC00847 in pancreatic adenocarcinoma (PAAD) samples. $^{*}p < 0.01$. **B** – The expression of LINC00847 in PC tissues and non-tumor tissues was assessed by RT-qPCR. **C** – The expression of LINC00847 in HuP-T3, Capam-1, PSN-1 and HPDE cells was detected by RT-qPCR, $^{**}p < 0.001$ compared to HPDE. **D** – The distribution of LINC00847 in the cytoplasm and nucleus was measured by RT-qPCR

MiR-455-3p, a direct target of LINC00847, blocks PC progression

The StarBase database showed that the LINC00847 sequence included the binding sites in miR-455-3p (Figure 5 A). Dual-luciferase reporter (DLR) analysis was carried out to evaluate the binding activity among miR-455-3p as well as LINC00847. Compared with LINC00847-MUT and miR-455-3p mimics co-transfected cells using one-way ANOVA, miR-455-3p mimics and LINC00847-WT co-transfected cells both showed significantly lower relative luciferase activity ($p < 0.001$, Figure 5 B). Evidently, LINC00847 silencing in Capan-1 and PSN-1 cells enhanced miR-455-3p expression ($p < 0.001$ using *t*-test, Figure 5 C). To examine the role of miR-455-3p in PC cells, we transfected miR-455-3p mimics into Capan-1 and PSN-1 cells. Increased miR-455-3p expression inhibited Capan-1 and PSN-1 cell invasion and proliferation compared to the mimic-NC group using the *t*-test ($p < 0.001$, Figures 5 D and E). According to the results, LINC00847 targeted miR-455-3p, and miR-455-3p mimics prevented progression of PC.

MiR-455-direct 3p's target gene is HDAC4

The results of the StarBase database showed where miR-455-3p and HDAC4 bind (Figure 6 A). Furthermore, HDAC4 was found to be overexpressed in PC tissues by RT-qPCR ($p < 0.0001$ using *t*-test, Figure 6 B). According to Western blot

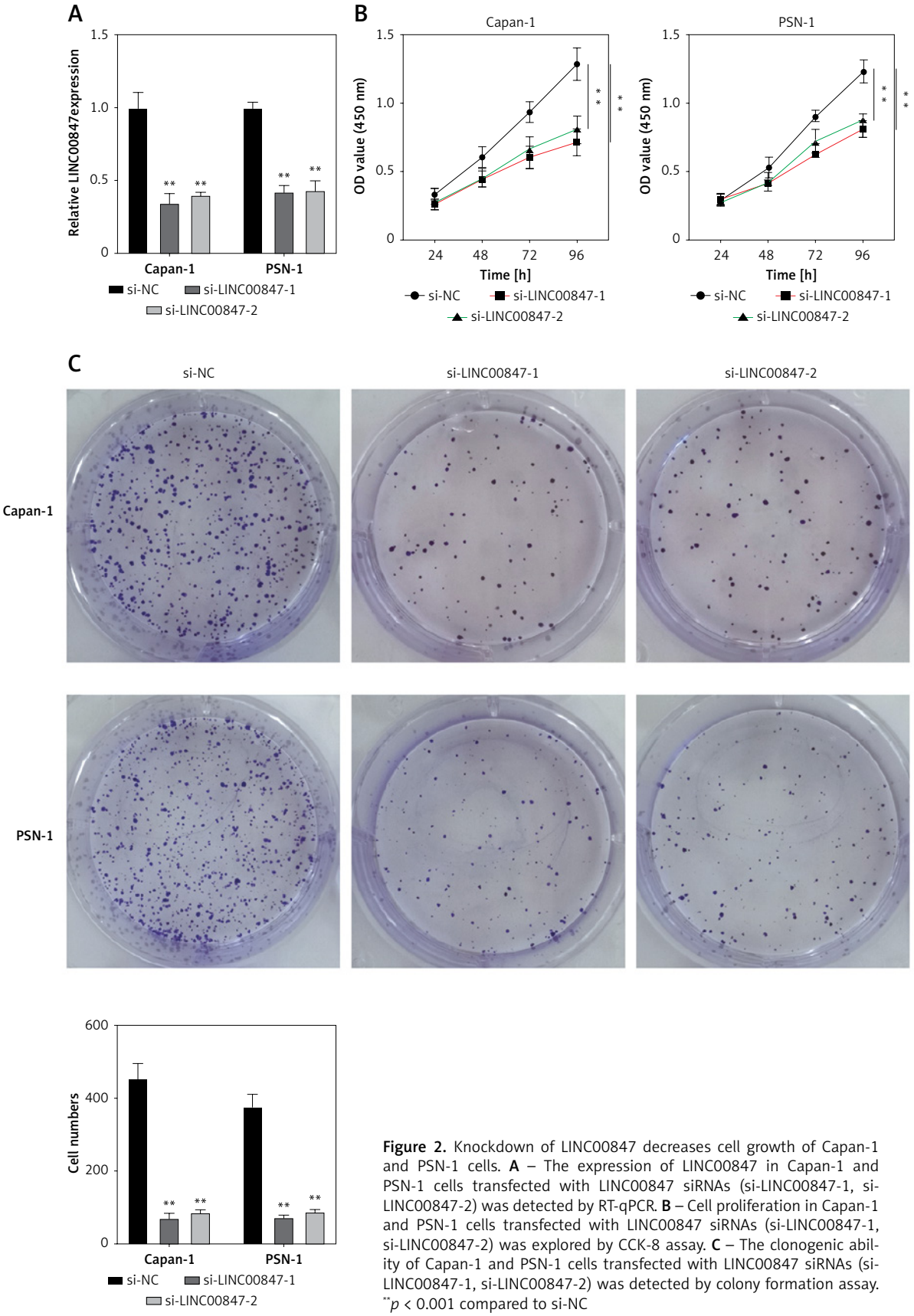

Figure 2. Knockdown of LINC00847 decreases cell growth of Capan-1 and PSN-1 cells. **A** – The expression of LINC00847 in Capan-1 and PSN-1 cells transfected with LINC00847 siRNAs (si-LINC00847-1, si-LINC00847-2) was detected by RT-qPCR. **B** – Cell proliferation in Capan-1 and PSN-1 cells transfected with LINC00847 siRNAs (si-LINC00847-1, si-LINC00847-2) was explored by CCK-8 assay. **C** – The clonogenic ability of Capan-1 and PSN-1 cells transfected with LINC00847 siRNAs (si-LINC00847-1, si-LINC00847-2) was detected by colony formation assay. $^{**}p < 0.001$ compared to si-NC

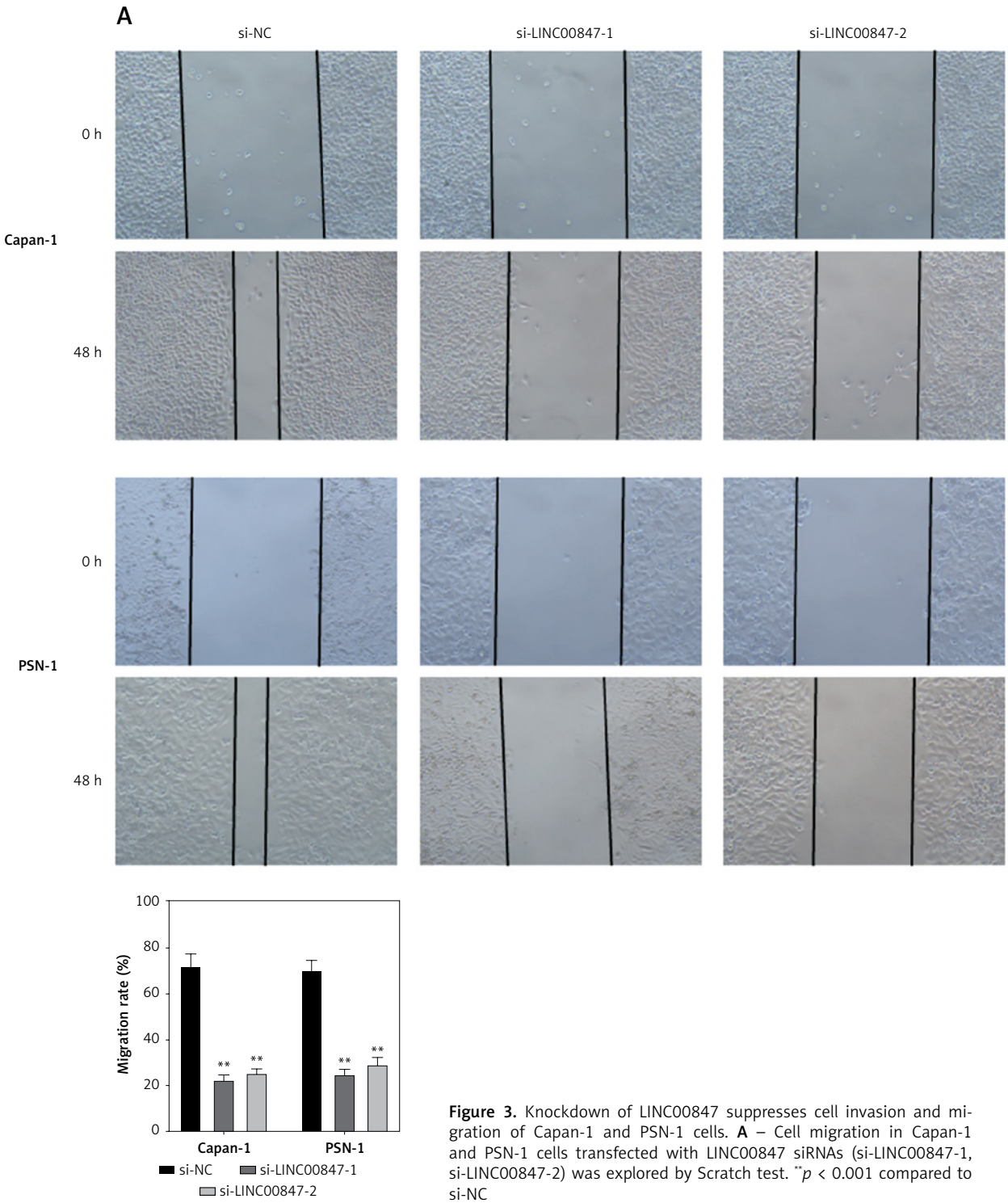

Figure 3. Knockdown of LINC00847 suppresses cell invasion and migration of Capan-1 and PSN-1 cells. **A** – Cell migration in Capan-1 and PSN-1 cells transfected with LINC00847 siRNAs (si-LINC00847-1, si-LINC00847-2) was explored by Scratch test. $^{**}p < 0.001$ compared to si-NC

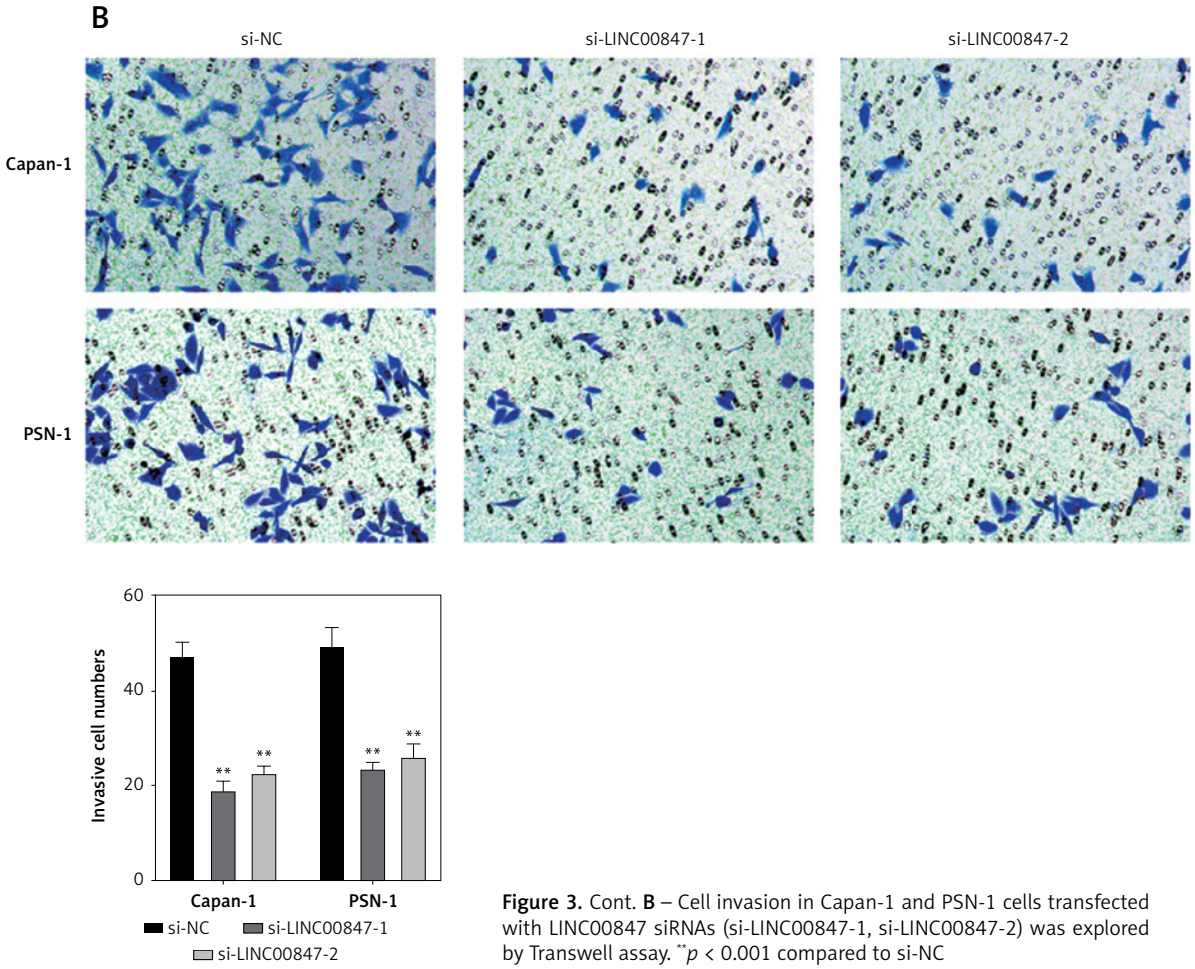

Figure 3. Cont. **B** – Cell invasion in Capan-1 and PSN-1 cells transfected with LINC00847 siRNAs (si-LINC00847-1, si-LINC00847-2) was explored by Transwell assay. $^{**}p < 0.001$ compared to si-NC

analysis, Capan-1 and PSN-1 cells expressed more HDAC4 protein than HPDE cells ($p < 0.001$ using one-way ANOVA, Figure 6 C). Notably, miR-455-3p mimics decreased HDAC4-WT's luciferase activity in Capan-1 and PSN-1 cells ($p < 0.001$ using one-way ANOVA, Figure 6 D). Furthermore, HDAC4 protein level was clearly decreased in Capan-1 as well as PSN-1 cells co-cultured with miR-455-3p mimics ($p < 0.001$ using *t*-test, Figure 6 E). According to the results of the Pearson's correlation analysis, the expression of LINC00847 and HDAC4 in PC tissues were positively associated (Figure 6 F) and inversely associated with miR-455-3p in PC tissues (Figure 6 G). Additionally, miR-455-3p and HDAC4 level of expression had a negative correlation (Figure 6 H). These outcomes suggested that miR-455-3p may have HDAC4 as a direct target gene.

HDAC4 overexpression reverses the effect of LINC00847 silencing

As shown in Figure 7 A, LINC0847 silencing suppressed HDAC4 expression, but HDAC4 overexpression disrupted the inhibition of IINC00847 silencing ($p < 0.001$, $p < 0.001$ using one-way ANOVA). Functionally, we found that HDAC4 overexpression revised the hindering effect of cell proliferation induced by LINC00847 silencing ($p < 0.001$ using one-way ANOVA, Figure 7 B). Additionally, LINC00847 silencing's inhibitory effect on the capacity for clonogenicity was lessened by HDAC4 overexpression ($p < 0.001$ using one-way ANOVA, Figure 7 C). HDAC4 overexpression also reduced the impact of LINC00847 silencing on the capacity of cells to invade and migrate ($p < 0.001$ using one-way ANOVA, Figures 7 D, E). Our data indicated that HDAC4 overexpression reversed the effect of LINC00847 silencing in PC.

Discussion

Recent studies have revealed that lncRNAs are closely related to the malignant progression of PC. For instance, lncRNA GSTM3TV2 enhanced gemcitabine resistance by reducing let-7 and increasing LAT2 and OLR1 in PC cells [16]. LINC00958 silencing blocked PC cell invasion and EMT progression by sponging miR-330-5p and reducing PAX8 [17]. Furthermore, lncRNA EPIC1 silencing reduced cell growth ability, and facilitated cell apoptosis and G1/S cell cycle arrest of PC cells [18]. We set out to look into the function of LINC00847 in the

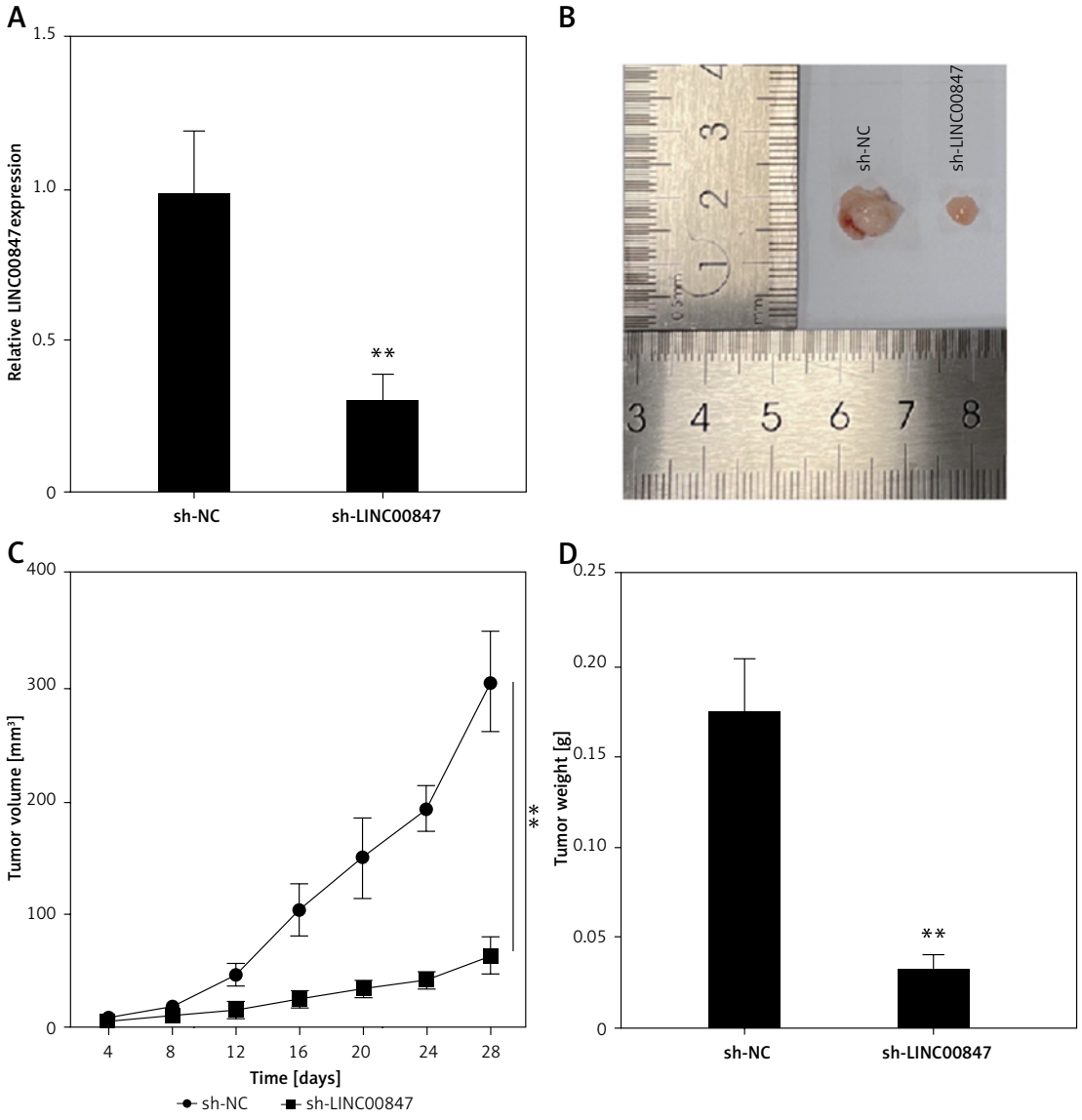

Figure 4. Knockdown of LINC00847 decreases tumor growth *in vivo*. **A** – The expression of LINC0847 in Capan-1 cells with sh-LINC00847 was detected by RT-qPCR. **B** – Images of tumors transfected with sh-LINC00847 and sh-NC. **C** – Every 4 days, the tumor volumes of the sh-LINC00847 group and sh-control group were measured. **D** – After 28 days, the tumor weights of the sh-LINC00847 group and sh-NC group were measured. $^{**}p < 0.001$ compared to sh-NC

tumor progression of PC. Previous research has shown that LINC00847 contributes to the development of various malignancies. In lung cancer, LINC00847 was upregulated and facilitated cell progression by modulating miR-147a and IFITM1 [9]. We discovered that PC cells and tissues have significant levels of LINC00847 expression. In particular, LINC00847 silencing reduced PC proliferation, invasiveness, as well as migration, and it also inhibited PC cell growth *in vivo*. These findings suggested that LINC00847 contributes to PC carcinogenesis.

LncRNAs have been confirmed to be a significant player in cancer progression by acting like sponges to absorb miRNAs. LINC00847 acted as an oncogenic factor in laryngeal squamous cell carcinoma by blocking miR-181a-5p and increasing ZEB2 expression [19]. In our study, we discovered that LINC00847 directly targeted miR-455-3p. It has been demonstrated that MiR-455-3p has varying impacts on the development of various malignancies. For instance, miR-455-3p expression was elevated in oral squamous cell carcinoma, and overexpression of miR-455-3p prevented the anticancer effects of LINC00472 [13]. In contrast, miR-455-3p prevented the progression of prostate cancer cells *in vitro* and *in vivo* [20]. Additionally, Zhan *et al.* reported that miR-455-3p mimic restrained cell multiplication of PANC1 as well as MIAPaCa2 cells [20]. Reduction of

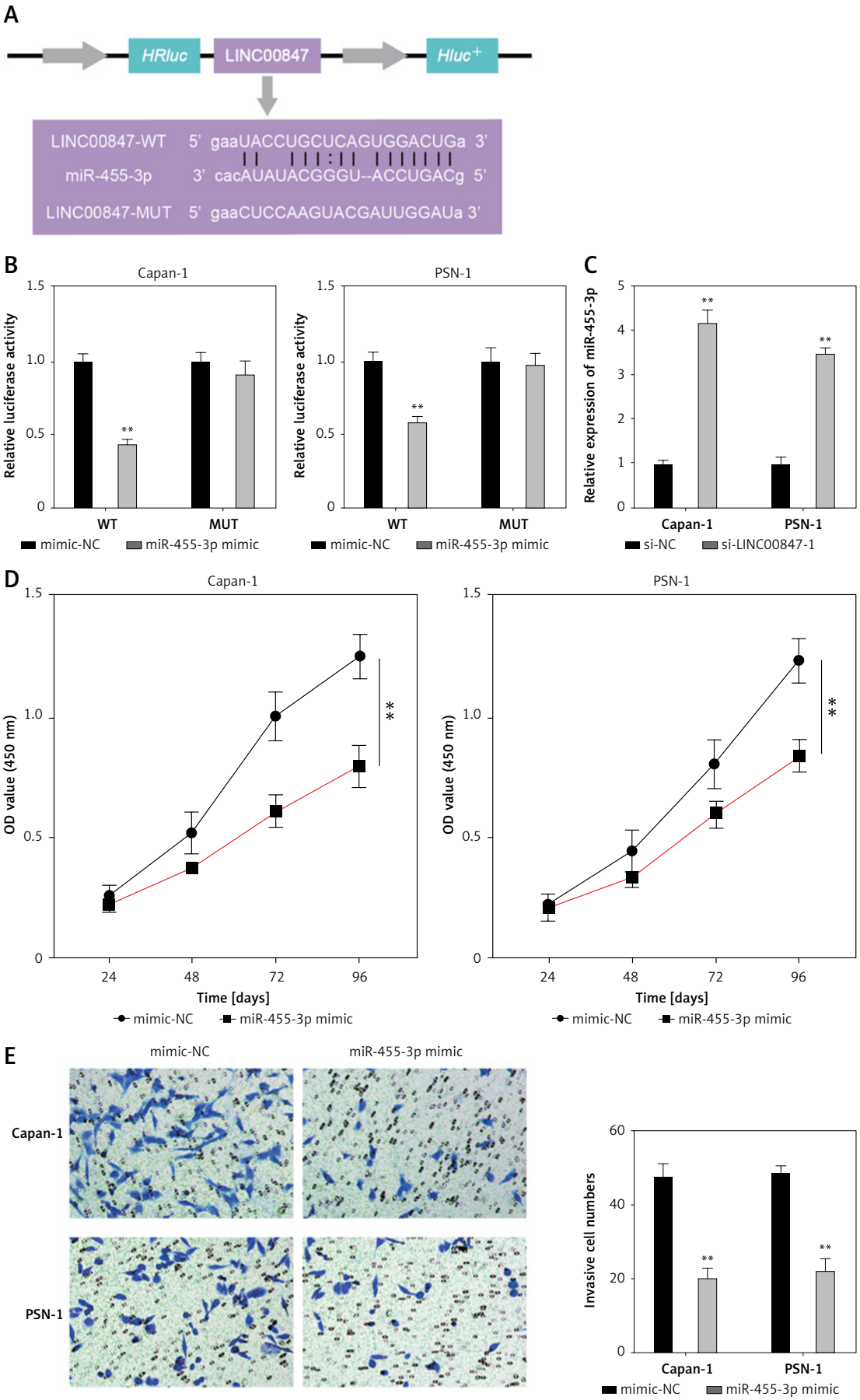

Figure 5. MiR-455-3p, a direct target of LINC00847, blocks PC progression. **A** – The binding sites between miR-455-3p and LINC00847 were predicted by StarBase. **B** – Dual-luciferase reporter assay was used to verify the relationship between LINC00847 and miR-455-3p, $^{**}p < 0.001$ compared to mimic-NC. **C** – The expression of miR-455-3p was detected by RT-qPCR, $^{**}p < 0.001$ compared to si-NC. **D** – Cell proliferation of Capan-1 and PSN-1 cells transfected with miR-455-3p mimic was detected by CCK-8 assay, $^{**}p < 0.001$ compared to mimic-NC. **E** – Cell invasion of Capan-1 and PSN-1 cells transfected with miR-455-3p mimics was detected by Transwell assay, $^{**}p < 0.001$ compared to mimic-NC

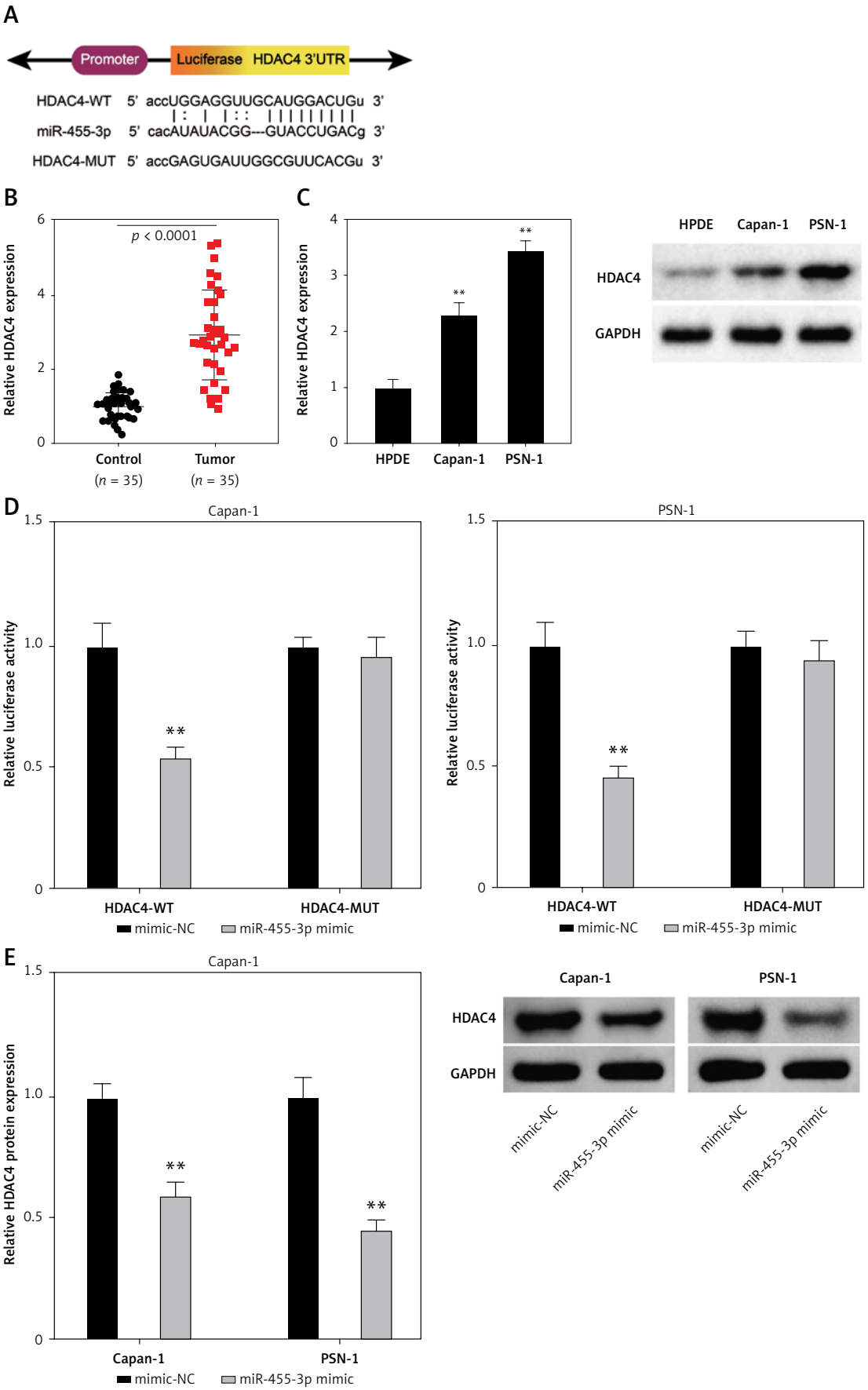

Figure 6. HDAC4 is a direct target gene of miR-455-3p. **A** – The matching sites between miR-455-3p and HDAC4 were predicted by StarBase. **B** – The mRNA expression of HDAC4 in PC tissues was examined by RT-qPCR, $^{**}p < 0.0001$ compared to control. **C** – The protein expression of HDAC4 in HPDE, Capan-1 and PSN-1 cells was detected by Western blot assay, $^{**}p < 0.001$ compared to HPDE cells. **D** – Dual-luciferase reporter assay was used to verify the relationship between HDAC4 and miR-455-3p, $^{**}p < 0.001$ compared to mimic-NC. **E** – The protein expression of HDAC4 in Capan-1 and PSN-1 cells transfected with miRR-455-3p mimics was measured by western blotting, $^{**}p < 0.001$ compared to mimic-NC

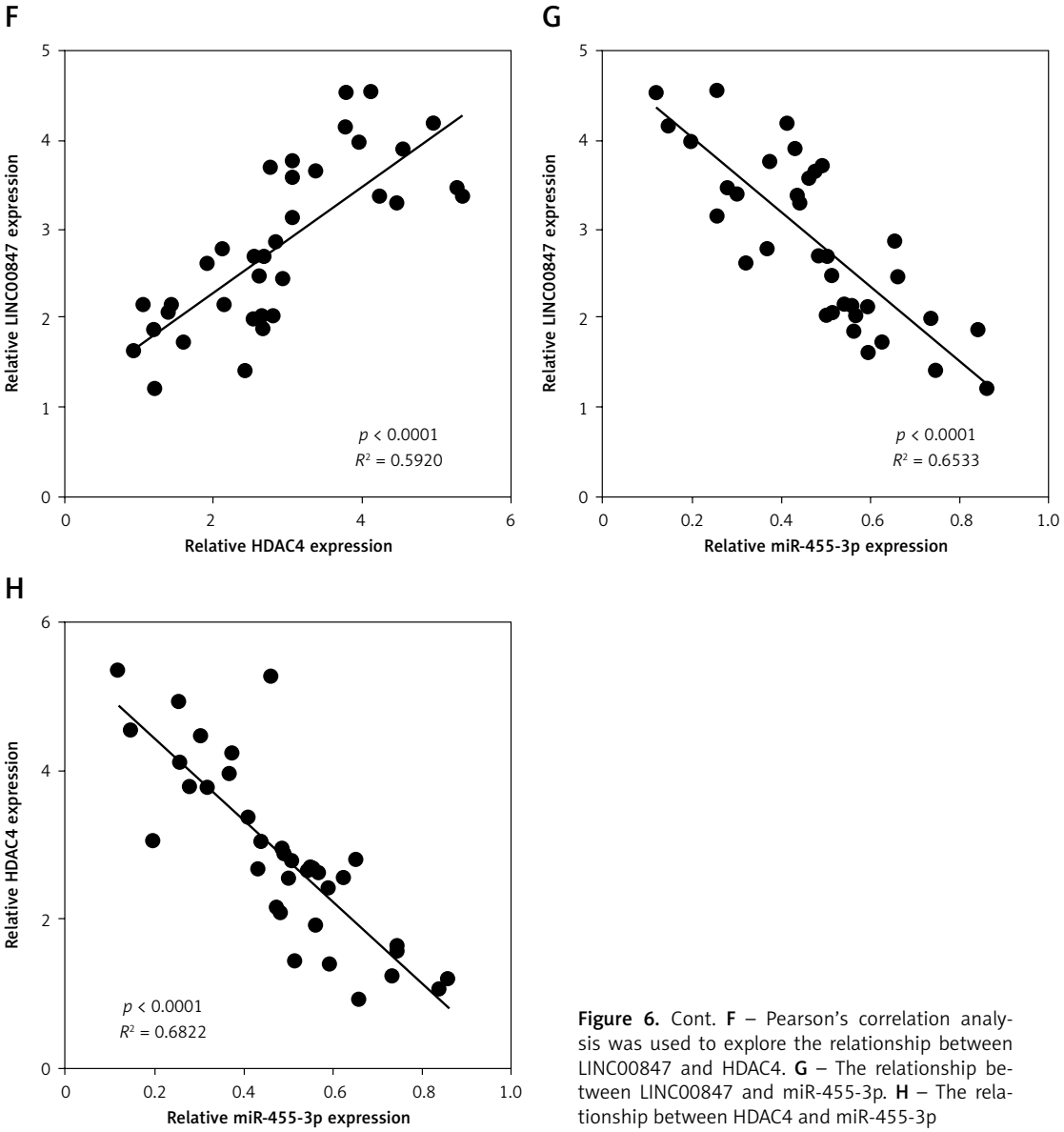

Figure 6. Cont. **F** – Pearson's correlation analysis was used to explore the relationship between LINC00847 and HDAC4. **G** – The relationship between LINC00847 and miR-455-3p. **H** – The relationship between HDAC4 and miR-455-3p

miR-455-3p accelerated cell invasion of SW1990 cells and PANC1 cells [21]. Similar to this, our findings indicated that miR-455-3p prevented Capan-1 cells and PSN-1 cells from proliferating and invading other cells. Our research as a whole demonstrated that miR-455-3p was a tumor-suppressing component in PC.

HDAC4, a key member of class IIa HDACs, is located in human chromosome 2q37.3 and expressed differently in different tissues and organs [22]. HDAC4 was verified to be a target of miR-455-3p. HDAC4 knockdown clearly suppressed cell proliferation of lung cancer cells [23]. Furthermore, HDAC4 acted as a tumor promoter in human multiple myeloma cells [24]. HDACs may be involved in the development of PC, where high expression of HDAC4 was borderline correlated with tumor growth and absent lymph node metastasis, and unrelated to organ metastasis [25]. Overexpression of HDAC4 was found in primary and metastatic pancreatic ductal adenocarcinoma [26]. We noted that HDAC4 was enhanced in PC tissues and cell lines, which is consistent with prior research. LINC00847 knockdown had an inhibitory impact on PC cells that was mechanically reduced by HDAC4.

The small number of patients is a limitation of this study. In future studies, we will increase the number of patients to validate the action of the LINC00847/miR-455-3p /HDAC4 axis in PC. More investigation is required to ascertain the mechanism by which miR-455-3p controls HDAC4 to promote PC cell growth.

In conclusion, this study confirms that LINC00847 is a tumor promoter in PC progression by sponging miR-455-3p to regulate HDAC4. Our findings provide a robust theoretical basis for potential therapeutic interventions targeting PC, highlighting the pivotal role of the LINC00847/

miR-455-3p/HDAC4 axis in the pathogenesis of this condition.

Acknowledgments

Shunxin Hao, Zhi Yao contributed equally to this work.

Funding

No external funding.

Ethical approval

The ethical committee of Wuhan University of Science and Technology Hospital accepted this study (Wuhan, China) (2021 S2897). For the processing of clinical tissue samples, we followed the ethical criteria of the Declaration of Helsinki. A consent form was signed by each patient.

The laboratory animal care and use guidance was followed in the execution of this animal experiment. The ethics committee of the Wuhan University of Science and Technology Hospital gave its approval for each procedure used in this investigation. The ARRIVE criteria were followed in all animal trials.

The participants agreed to publication. A formal written informed consent form was signed by each patient.

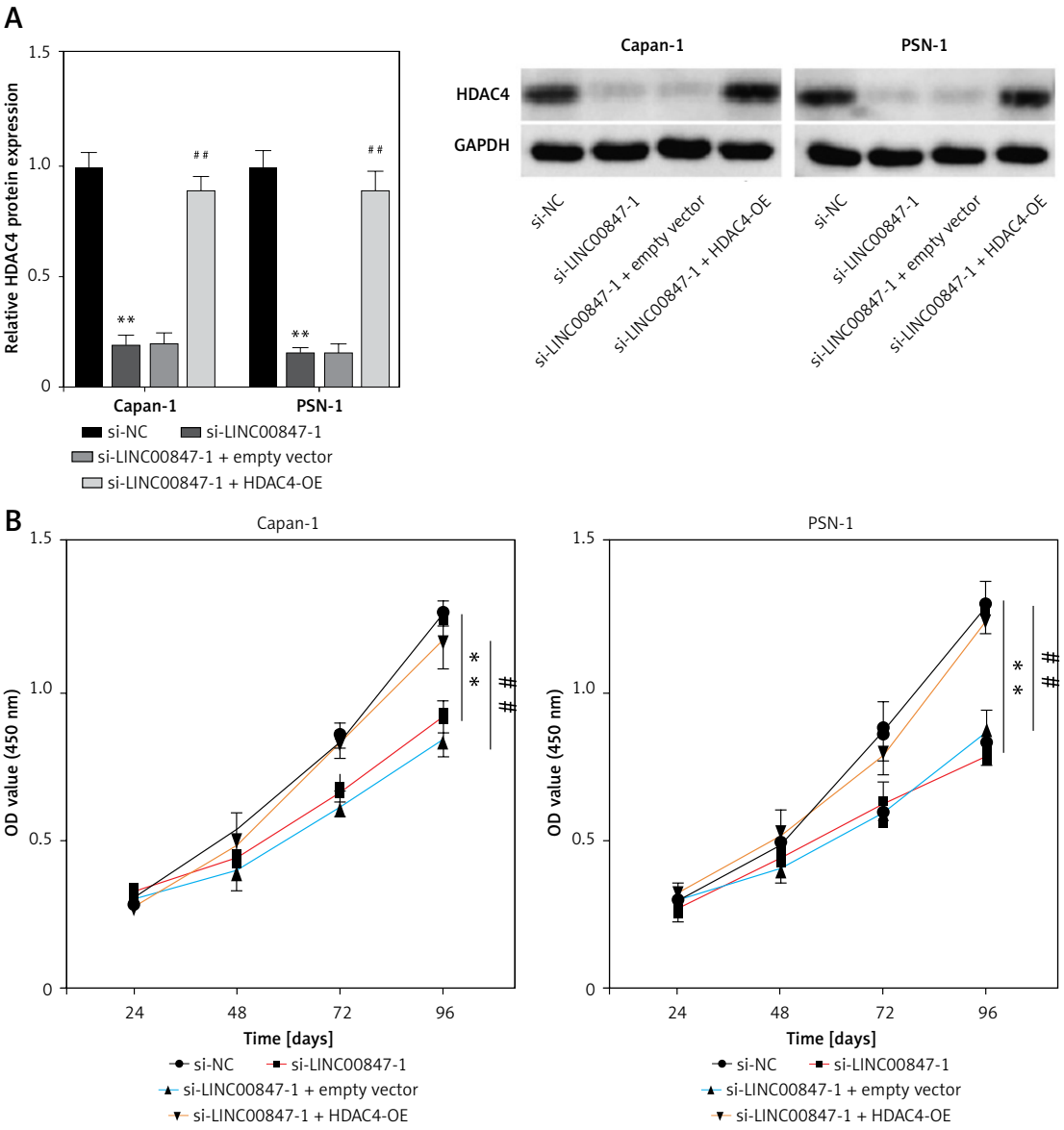

Figure 7. HDAC4 overexpression reverses the effect of LINC00847 silencing on PC cells. **A** – The protein expression of HDAC4 in Capan-1 and PSN-1 cells transfected with LINC00847 silencing was detected by Western blot assay. **B** – Cell proliferation of Capan-1 and PSN-1 cells was detected by CCK-8 assay

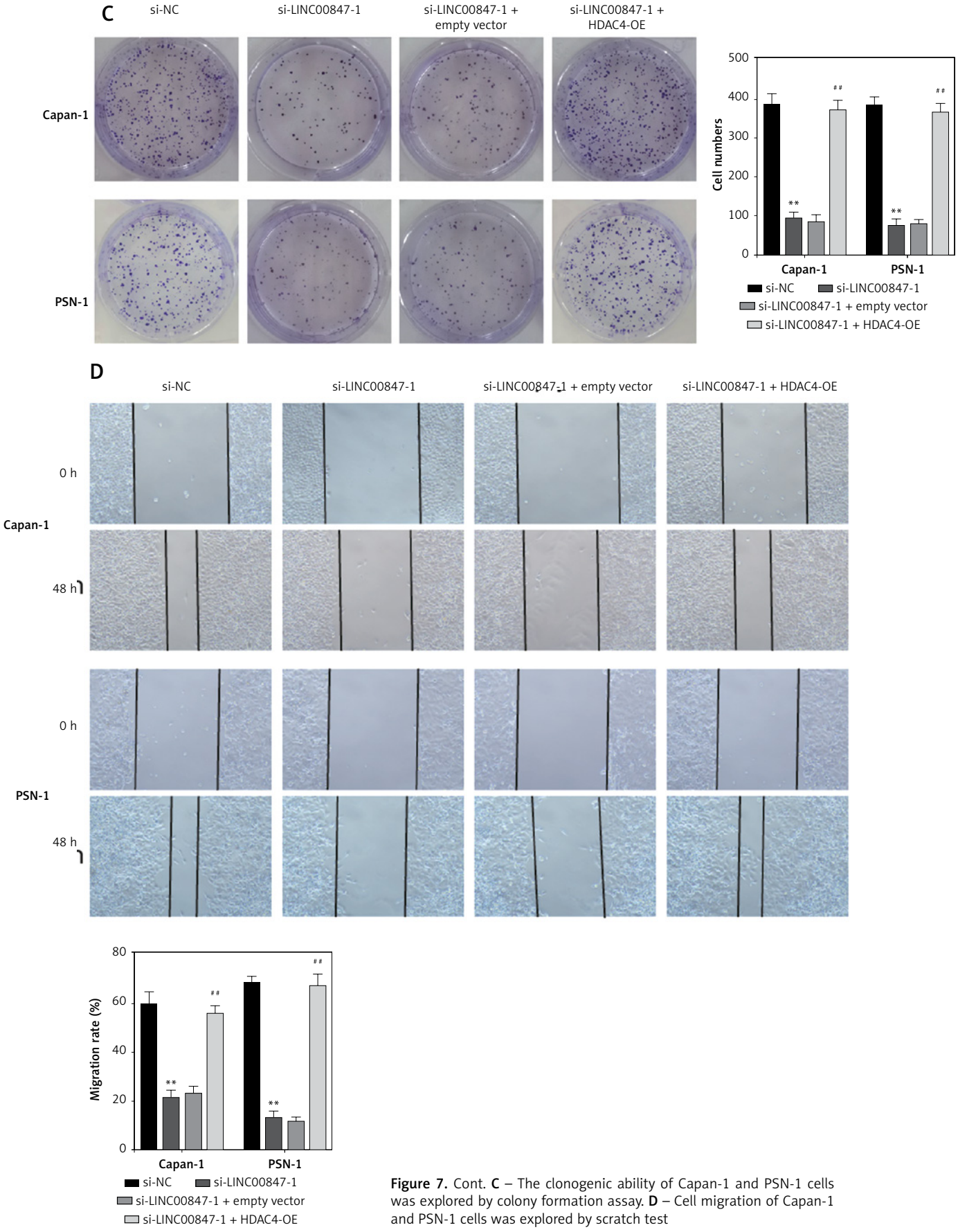

Figure 7. Cont. **C** – The clonogenic ability of Capan-1 and PSN-1 cells was explored by colony formation assay. **D** – Cell migration of Capan-1 and PSN-1 cells was explored by scratch test

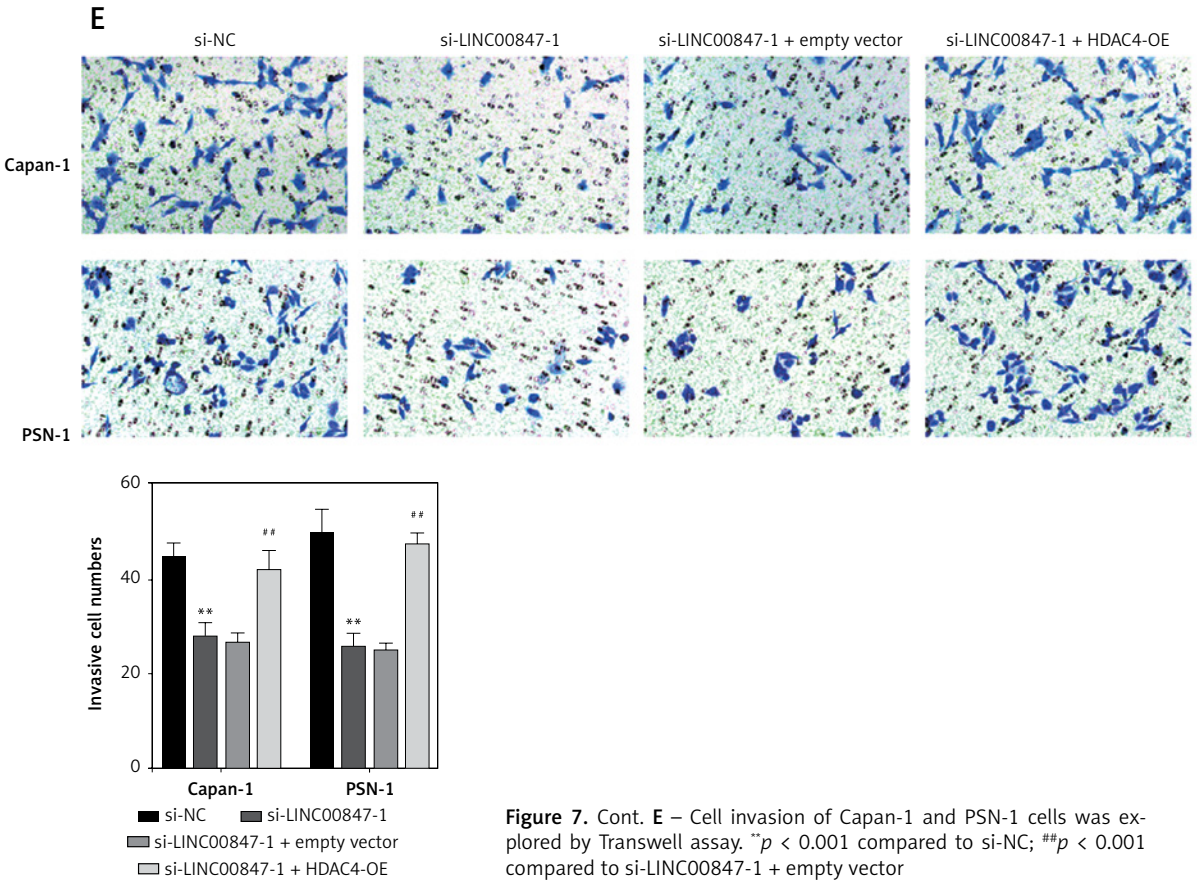

Figure 7. Cont. **E** – Cell invasion of Capan-1 and PSN-1 cells was explored by Transwell assay. $^{**}p < 0.001$ compared to si-NC; $^{\#\#}p < 0.001$ compared to si-LINC00847-1 + empty vector

Conflict of interest

The authors declare no conflict of interest.

References

1. Sung H, Ferlay J, Siegel RL, et al. Global Cancer Statistics 2020: GLOBOCAN estimates of incidence and mortality worldwide for 36 cancers in 185 countries. CA Cancer J Clin 2021; 71: 209-49.
2. Strobel O, Neoptolemos J, Jäger D, Büchler MW. Optimizing the outcomes of pancreatic cancer surgery. Nat Rev Clin Oncol 2019; 16: 11-26.
3. Siegel RL, Miller KD, Jemal A. Cancer statistics, 2020. CA Cancer J Clin 2020; 70: 7-30.
4. Wright MW, Bruford EA. Naming 'junk': human non-protein coding RNA (ncRNA) gene nomenclature. Hum Genom 2011; 5: 90-8.
5. Yang M, Lu H, Liu J, Wu S, Kim P, Zhou X. lncRNAfunc: a knowledgebase of lncRNA function in human cancer. Nucleic Acids Res 2022; 50: D1295-306.
6. Li H, Wang X, Wen C, et al. Long noncoding RNA NORAD, a novel competing endogenous RNA, enhances the hypoxia-induced epithelial-mesenchymal transition to promote metastasis in pancreatic cancer. Mol Cancer 2017; 16: 169.
7. Zhu H, Shan Y, Ge K, Lu J, Kong W, Jia C. LncRNA CYTOR promotes pancreatic cancer cell proliferation and migration by sponging miR-205-5p. Pancreatology 2020; 20: 1139-48.
8. Zhang M, Wang R, Zhao X, Lu L, Wang T. LncRNA LINK-A regulates ROCK1 expression in early-stage pancreatic adenocarcinoma. Exp Ther Med 2020; 19: 1933-39.
9. Li H, Chen YK, Wan Q, et al. Long non-coding RNA LINC00847 induced by E2F1 accelerates non-small cell lung cancer progression through targeting miR-147a/IFITM1 axis. Front Med (Lausanne) 2021; 8: 663558.
10. Tu LR, Li W, Liu J, Song XG, Xu HW. LncRNA LINC00847 contributes to hepatocellular carcinoma progression by acting as a sponge of miR-99a to induce E2F2 expression. J Biol Regul Homeost Agents 2020; 34: 2195-203.
11. Si L, Yang Z, Ding L, Zhang D. Regulatory effects of lncRNAs and miRNAs on the crosstalk between autophagy and EMT in cancer: a new era for cancer treatment. J Cancer Res Clin Oncol 2022; 148: 547-64.
12. Sharma GG, Okada Y, Von Hoff D, Goel A. Non-coding RNA biomarkers in pancreatic ductal adenocarcinoma. Semin Cancer Biol 2021; 75: 153-68.
13. Liu X, Ma X, Li H, et al. LINC00472 suppresses oral squamous cell carcinoma growth by targeting miR-455-3p/ELF3 axis. Bioengineered 2022; 13: 1162-73.
14. Sun F, Yu Z, Wu B, Zhang H, Ruan J. LINC00319 promotes osteosarcoma progression by regulating the miR-455-3p/NFIB axis. J Gene Med 2020; 22: e3248.
15. Zhan T, Zhu Q, Han Z, et al. miR-455-3p functions as a tumor suppressor by restraining Wnt/β-catenin signaling via TAZ in pancreatic cancer. Cancer Manag Res 2020; 12: 1483-92.
16. Xiong G, Liu C, Yang G, et al. Long noncoding RNA GSTM3TV2 upregulates LAT2 and OLR1 by competitively sponging let-7 to promote gemcitabine resistance in pancreatic cancer. J Hematol Oncol 2019; 12: 97.

17. Chen S, Chen JZ, Zhang JQ, et al. Silencing of long noncoding RNA LINC00958 prevents tumor initiation of pancreatic cancer by acting as a sponge of microRNA-330-5p to down-regulate PAX8. Cancer Lett 2019; 446: 49-61.
18. Xia P, Liu P, Fu Q, et al. Long noncoding RNA EPIC1 interacts with YAP1 to regulate the cell cycle and promote the growth of pancreatic cancer cells. Biochem Biophys Res Commun 2020; 522: 978-85.
19. Li W, Hu X, Huang X. Long intergenic non-protein coding RNA 847 promotes laryngeal squamous cell carcinoma progression through the microRNA-181a-5p/zinc finger E-box binding homeobox 2 axis. Bioengineered 2022; 13: 9987-10000.
20. Zhao Y, Yan M, Yun Y, et al. MicroRNA-455-3p functions as a tumor suppressor by targeting eIF4E in prostate cancer. Oncol Rep 2017; 37: 2449-58.
21. Zhu J, Zhou Y, Zhu S, et al. circRNA circ_102049 implicates in pancreatic ductal adenocarcinoma progression through activating CD80 by targeting miR-455-3p. Mediators Inflamm 2021; 2021: 8819990.
22. Wen Y, Li B, He M, Teng S, Sun Y, Wang G. circHIPK3 promotes proliferation and migration and invasion via regulation of miR-637/HDAC4 signaling in osteosarcoma cells. Oncol Rep 2021; 45: 169-79.
23. Jin K, Zhao W, Xie X, Pan Y, Wang K, Zhang H. MiR-520b restrains cell growth by targeting HDAC4 in lung cancer. Thorac Cancer 2018; 9: 1249-54.
24. Ma H, Shen L, Yang H, Gong H, Du X. Circular RNA circPSAP functions as an efficient miR-331-3p sponge to regulate proliferation, apoptosis and bortezomib sensitivity of human multiple myeloma cells by upregulating HDAC4. J Pharmacol Sci 2022; 149: 27-36.
25. Giaginis C, Damaskos C, Koutsounas I, et al. Histone deacetylase (HDAC)-1, -2, -4 and -6 expression in human pancreatic adenocarcinoma: associations with clinicopathological parameters, tumor proliferative capacity and patients' survival. BMC Gastroenterol 2015; 15: 148.
26. Yang J, Chheda C, Lim A, et al. HDAC4 mediates smoking-induced pancreatic cancer metastasis. Pancreas 2022; 51: 190-95.